Supporting Information (SI)

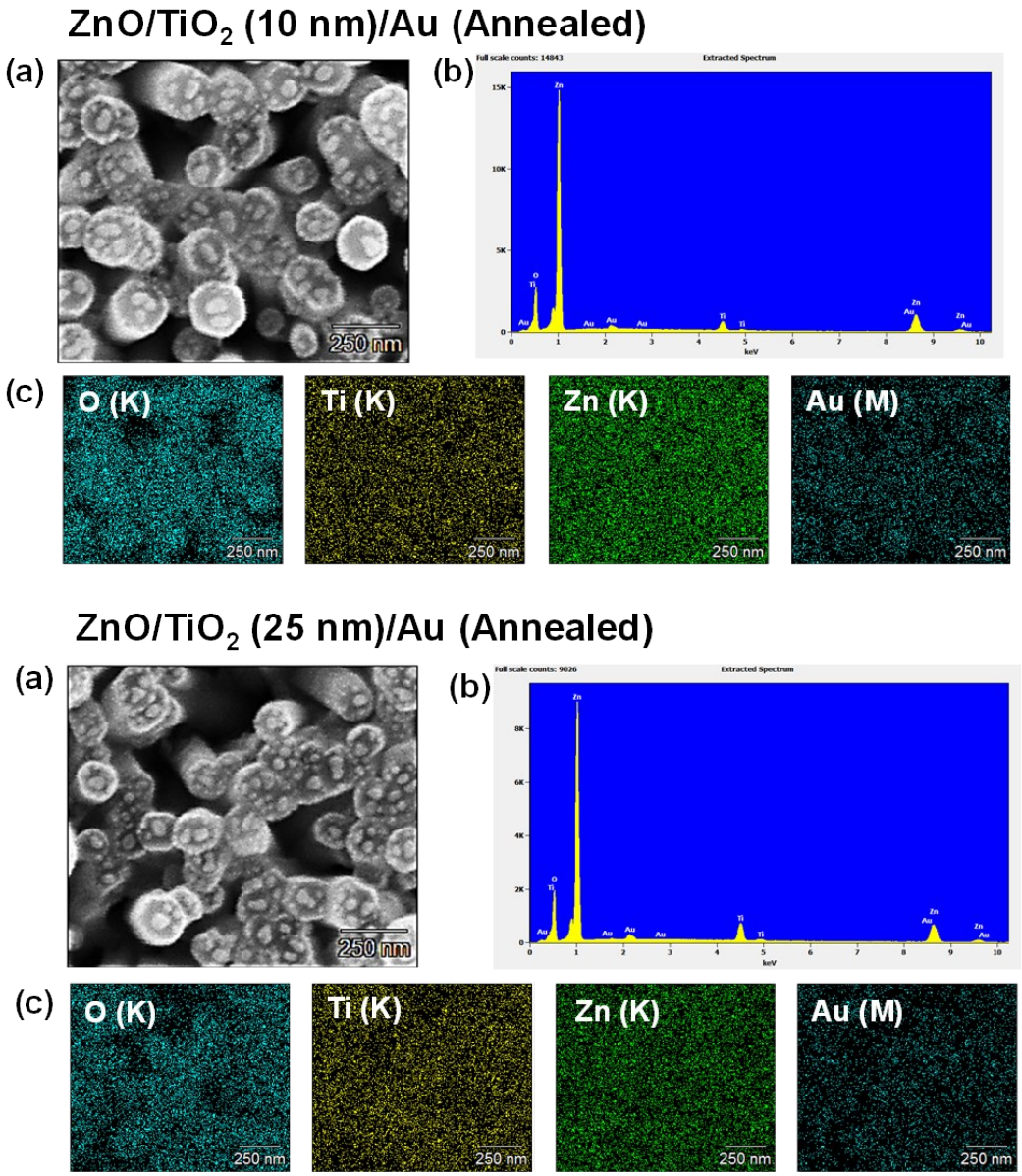

Fig. S1 EDS results of ZnO/TiO_2 core-shell NRs with a different shell thickness decorated with the plasmonic Au NPs. (a), (d) SEM images, and (b), (e) EDS. (c) and (f) EDS element mapping data of O, Ti, Zn, and Au.

Element	ZnO/TiO_2 (10 nm)/Au		ZnO/TiO_2 (25 nm)/Au	
	Weight (%)	Atomic (%)	Weight (%)	Atomic (%)
O K	17.68	46.82	18.84	48.34
Ti k	5.70	5.04	10.19	8.73
Zn L	73.12	47.39	67.08	42.12
Au M	3.50	0.75	3.09	0.81
Totals	100	100	100	100

Table S1. Weight and atomic values of a ZnO/TiO_2 core-shell NRs with the different shell thickness decorated with the plasmonic Au NPs.

Fig. S1 and Table S1. show the SEM images, EDS spectrum, and EDS elemental mapping data. Through the results of EDS analysis, we can find each samples consist of Zn, Ti, O, and Au. Furthermore, weight and atomic % of Ti and O were increased with the TiO_2 thickness. This result shows the thickness of the TiO_2 layer is controlled according to the synthesis time.

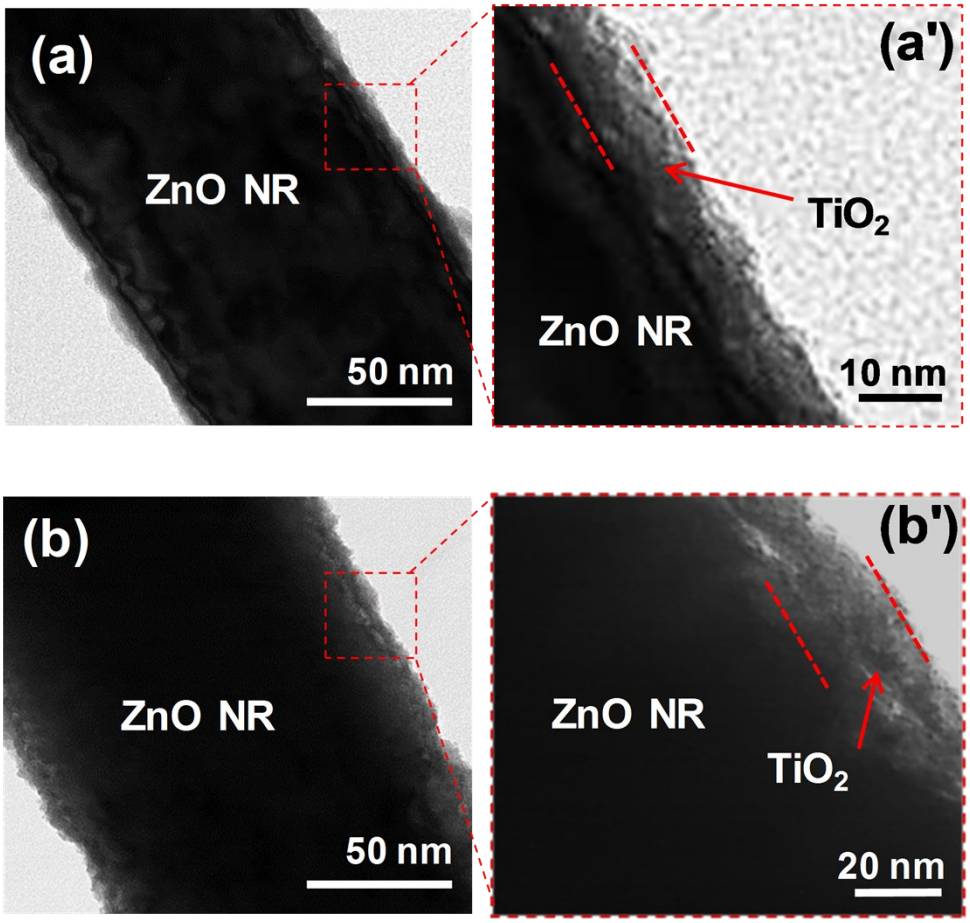

Fig. S2 (a), (b) Low and (a'), (b') high-magnification of TEM images of ZnO/TiO_2 core-shell nanorods with the 10 nm and 25 nm-thick TiO_2 shell layer, respectively.[1-3]

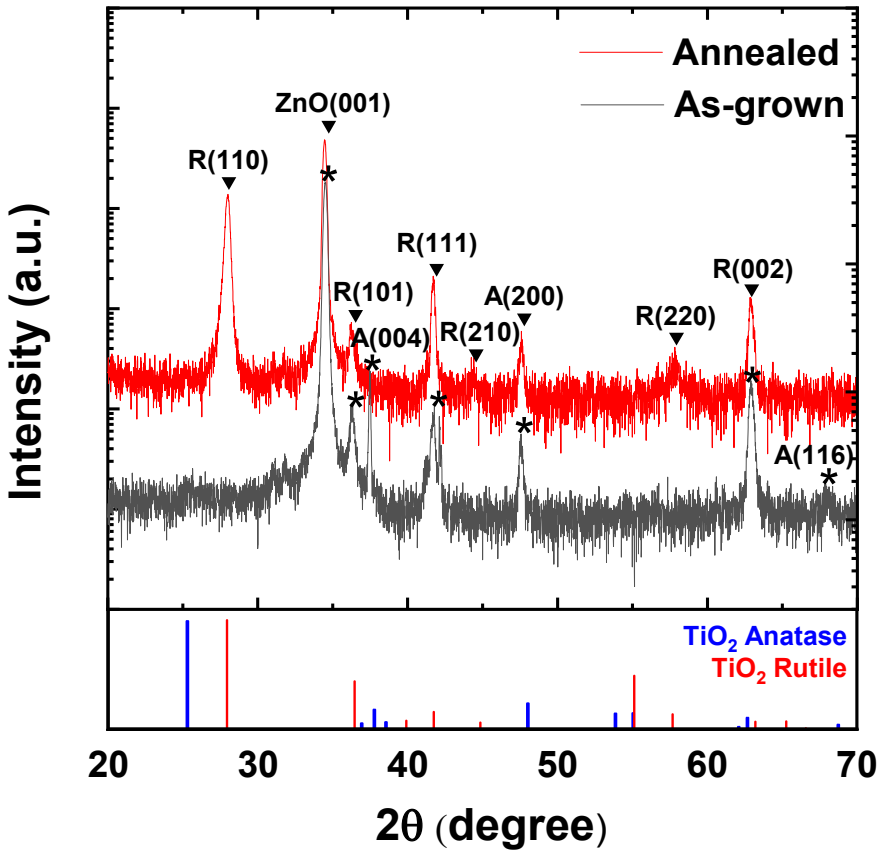

Fig. S3 X-ray diffraction results of ZnO/TiO_2 core-shell NRs before and after annealing process at 500 °C with the standard cards of anatase and rutile TiO_2.

As shown this Fig S3., we can confirm the TiO_2 shell layer was crystalized from amorphous (anatase) to rutile.

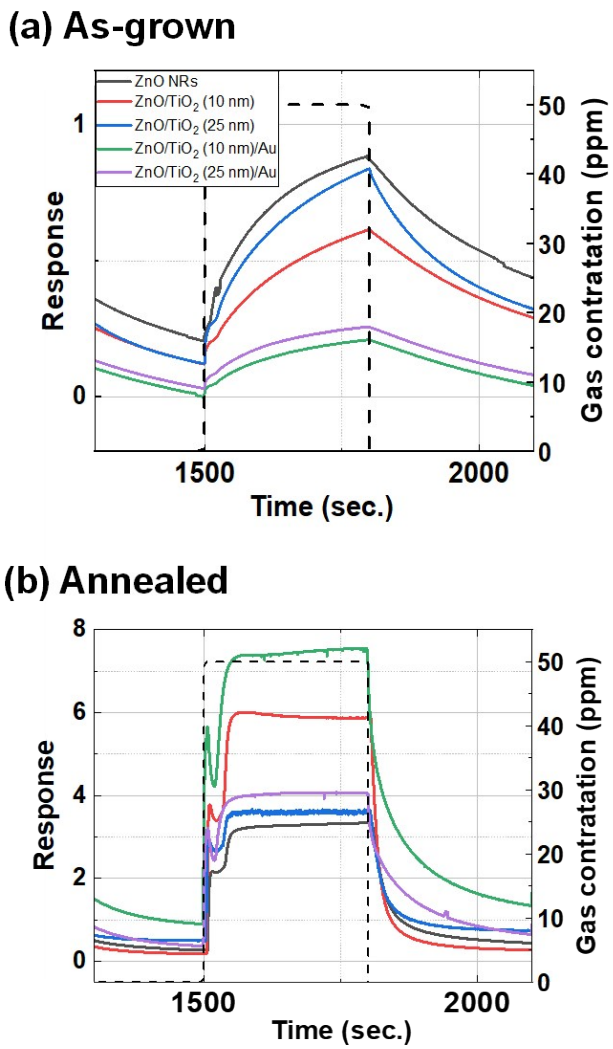

Fig. S4 Response of gas sensors at 50 ppm of NO_2 gas concentration with the UV irradiation. (a) As-grown and (b) annealed gas sensors.

Element	As-grown		Annealed	
	T_s (sec.)	T_r (sec.)	T_s (sec.)	T_r (sec.)
ZnO NRs	210	245	48	100
ZnO/TiO_2 (10 nm)	240	252	43	50
ZnO/TiO_2 (25 nm)	226	230	40	74
ZnO/TiO_2 (10 nm)/Au	225	258	45	148
ZnO/TiO_2 (25 nm)/Au	225	256	42	162

Table S2. T_s and T_r values of gas sensors at 50 ppm of NO_2 gas concentration with UV irradiation.

Fig. S4 and Table S2. show the response (T_s) and recovery (T_r) time of gas sensors. In Fig. S2, we can see the annealed gas sensor graphs are steeper than as-grown gas sensors. This is like the annealed one have a faster response and recovery times than as-grown one due to the enhanced electrical properties of ZnO NRs and high crystallinity of TiO_2 shell layer through the annealing process.[28] Furthermore, in Table S2., the annealed gas sensors with a TiO_2 shell layer deposited on the ZnO NRs have the fastest response and recovery time than others. However, the Au layer deposited to the gas sensors show the slow-down recovery time. It is due to the UV light absorption in Au layer as explained in our manuscript.

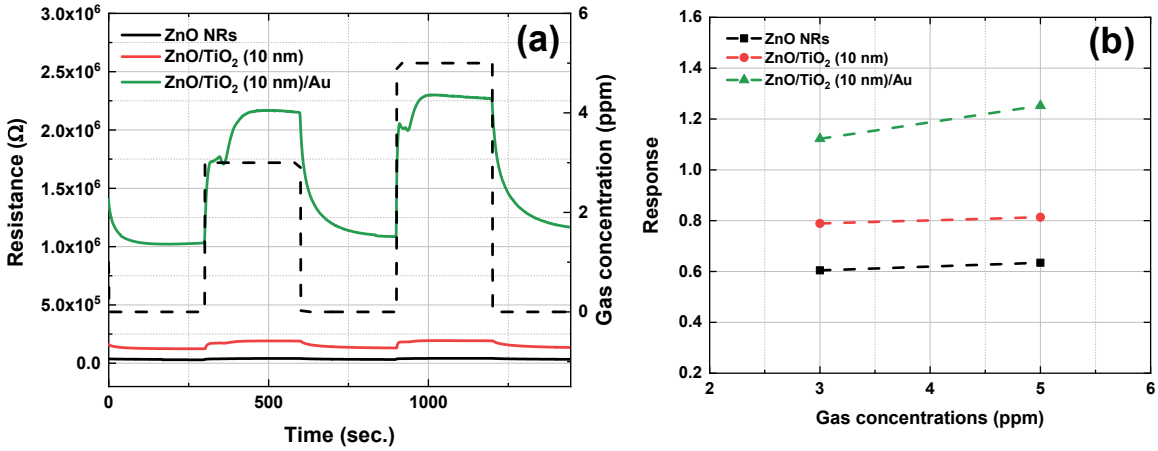

Fig. S5 (a) Resistance of annealed gas sensors with UV irradiation as a 3 and 5 ppm of NO_2 gas concentrations. (b) Response values of gas sensors as NO_2 gas concentrations of 3 and 5 ppm, respectively.

The gas sensor fabricated with ZnO/TiO_2 (10 nm) core-shell nanorods decorated with Au nanoparticles also show the highest response than the ZnO/TiO_2 (10 nm) core-shell NRs and ZnO NRs at the 3 and 5 ppm of NO_2 gas concentrations.

References

[1] Y. Xu, L. Zheng, C. Yang, W. Zheng, X. Liu, and J. Zhang, *Sens. Actuator B-Chem.*, 2020, **310**, 127846.

[2] F. Kayaci, S. Vempati, C. Ozgit-Akgun, I. Donmez, N. Biyikli, T. Uyar, *Nanoscale*, 2014, **6**, 5735.

[3] S. Panigrahi, D. Basak, *Nanoscale*, 2011, **3**, 2336.